REVIEW

Applications of Light Scattering in Microbiology

STEPHEN E. HARDING

*Department of Applied Biochemistry and Food Science, University of Nottingham,
Sutton Bonington LE12 5RD, United Kingdom*

Applications of the three principal light scattering techniques of turbidimetry, differential light scattering, and quasi-elastic light scattering to systems of microorganisms are reviewed. The relation between the three techniques is demonstrated and it is shown how these techniques can yield basic structural, optical, and even hydrodynamic properties for a wide range of microorganisms, with particular emphasis on changes in such properties. Such applications include antibiotic susceptibility testing, the effects of inhibitors on trypanosome motility, spore structure, virus self-assembly, and bacterial motility on the surface of fermentation reactors. © 1986 Academic Press, Inc.

Contents. 1. *Introduction.* 2. *Turbidimetry.* 2.1. Application to viruses. 2.2. Application to bacteria. 3. *Differential light scattering (DLS).* 3.1. Application to viruses. 3.2. Application to bacteria. 4. *Quasi-elastic light scattering (QLS).* 4.1. Application to viruses. 4.2. Application to bacterial spores. 4.3. Application to motile microorganisms.

1. INTRODUCTION

For four decades light scattering techniques have been powerful, though difficult to use, tools for elucidating the conformation of biomolecular systems in solution. Such techniques, involving the elastic or quasi-elastic scattering of visible radiation have been applied mainly to the study of the mass and the gross conformation of biological macromolecules in solution. For example, a widely used light scattering experiment has been the "Zimm plot" method which has been used to determine the molecular weight, radius of gyration, and second virial coefficient of a wide range of biopolymers (see, e.g., Ref. (1)).

The theory which describes scattering by larger particles (i.e., those whose maximum dimension is of the same order as the wavelength of the incident light)—such as macromolecular assemblies—is more complex, because of intramolecular interference effects. On the other hand, precisely because of such interference, it is (in principle at least) possible to obtain more detailed information about the gross morphology and internal structure of such assemblies. Large particle scattering also affords the advantage of greater signal to noise ratios: this means that difficulties caused by the presence (and removal) of dust and other particles in macromolecular suspensions are not so serious, and in addition that a sufficient signal can be obtained in shorter time intervals.

The intention of this review is to alert biochemists and microbiologists to recent advances in light scattering techniques and to illustrate recent and potential applications to microbiological systems: such applications are as diverse as the study of bacteriophage self-assembly, heat resistance of bacterial spores, trypanosome motility, biological wastewater monitoring, and fermenter contaminations. It is not the intention of this review to provide a complete treatise on the theory of light scattering—such material can be found in the many standard texts available (see, e.g., Refs. (2–8)) and reviews (9–14).

The first collection of laser light scattering papers devoted exclusively to biological and medical applications appeared in 1982 ("Biomedical Applications of Laser Light Scattering," Sattelle *et. al.*, eds., Elsevier). More recently, an excellent series of short papers, describing applications of laser light scattering to a range of biochemical systems, has appeared in Biochemical Society Transactions 1984, **12,** 623–627. Nevertheless, as far as I am aware no review to date has focused exclusively on the applications of a range of light scattering techniques to microbiology.

A limited amount of the relevant theory is given here, sufficient to demonstrate to the biochemist or microbiologist how turbidimetry, differential light scattering (DLS),[1] and quasi-elastic light scattering (QLS) are related and how they can provide complementary information on a particular system of microorganisms. This review will not cover the application of related techniques, such as electric birefringence, electrophoretic light scattering, or the circular dichroism of light scatterers: examples of the application of these techniques to microbiology can be found elsewhere (15–17).

2. TURBIDIMETRY

This is perhaps the simplest type of light scattering measurement to be made since to determine the "turbidity" of a suspension the total loss of intensity is measured through scattering of the incident beam, using a conventional spectrophotometer: it can be regarded therefore as a "zero scattering angle" measurement. If the refractive index increment can also be measured (by using for example a differential refractometer), turbidity then provides a convenient way for measuring the relative molecular mass, M_r, of macromolecular assemblies (with $M_r \gtrsim 10^6$) (17, 18) including viruses (19, 20, 22) and bacteria (21).

The turbidity of a suspension is defined as the fractional loss of intensity I of an incident beam by *scattering* per unit pathlength (x) of the suspension:

$$\tau = \frac{-(dI/dx)}{I}.$$ [1]

τ can be related to the "optical density" (OD) via

$$\tau = 2.303 \cdot (OD).$$ [2]

The turbidity is normally measured relative to the suspending medium or solvent and can be related to the M_r of the scatterer via

---

[1] Abbreviations used: DLS, differential light scattering; QLS, quasi-electric light scattering; OD, optical density; RGD, Rayleigh–Gans–Debye; TYMV, turnip yellow mosaic virus; BAC, bromo-acetyl carnitine; TMV, tobacco mosaic virus.

$$\tau = M_r \cdot c \cdot H \cdot Q(\lambda) \tag{3}$$

where

$$H = 32\pi^3 (\partial n/\partial c)^2 / 3 N_A \lambda_0^4. \tag{4}$$

In these equations c is the concentration (g/ml), n the refractive index, N_A Avogadro's number, λ_0 the wavelength *in vacuo*, and Q the particle dissipation factor (17); that is, a dimensionless number between 0 and 1 which depends on the dimensions of the scattering particle relative to the wavelength through the medium, λ:

$$Q = \frac{3}{8} \int_0^\pi P(\theta)(1 + \cos^2 \theta)\sin \theta d\theta \tag{5}$$

where θ is the scattering angle and $P(\theta)$ is the ratio of the actual scattered intensity of a particle to the scattered intensity without interference. The $P(\theta)$ values—and hence Q values for a wide range of particle shapes—have been worked out by Doty and Steiner (17) based on the assumption that contributions from $P(\theta)$ are solely from intraparticle interference effects and that there are no significant changes in phase of the light passing through the particle (this is known as the Rayleigh–Gans–Debye (RGD) approximation). Camerini-Otero and Day (22) have used a series expansion for $P(\theta)$ given by Debye (18) to produce a general expression for Q for any shape of scatterer

$$Q = 1 - \sum_{n-1}^\infty (-1)^{n+1} \cdot q_{2n} \left(\frac{4\pi d}{\lambda}\right)^{2n} \tag{6}$$

where d is its "principal dimension" (viz., length for a rod, radius for a sphere, or the root mean square end-to-end distance for a random coil) and the coefficients q_{2n} have been tabulated, enabling simple computer evaluations of Q.

When the shape of a scatterer is *not* known an estimate for Q can be obtained from the wavelength dependence of the turbidity (17, 19):

$$\frac{-d \log \tau}{d \log \lambda_0} = 4 - \beta \tag{7}$$

where $\beta = (d \log Q/d \log \lambda_0)$. β can therefore be *estimated* from a double logarithmic plot of τ vs λ_0. Once β is determined, Q can be obtained from the tables of Doty and Steiner (17). The assumption is of course made that loss of intensity is due to scattering and not absorbance. This method of determining the molecular weight after allowance for intraparticle interference (via Q) is only rigorous in the absence of interparticle interference effects: strictly speaking the "apparent M_r" measured at a finite concentration needs to be extrapolated to infinite dilution, which is why Eq. [3] is often rewritten in the form

$$\frac{1}{M_r} = HQ \lim_{c \to 0} \left(\frac{c}{\tau}\right). \tag{8}$$

2.1 Application to Viruses

Although, as a means of determining molecular weights of most *macromolecules* of biological interest, turbidimetry has been of limited use (because of the relatively low scattering), for particles of $M_r \gtrsim 10^6$—which includes viruses—it provides a valu-

TABLE I

Molecular Weights of Viruses Determined by Turbidimetry

Virus	$10^{-6} \times M_r$		Ref.
	Turbidimetry	Other	
R17	3.86 ± 0.37	3.80 ± 0.23^a	
		3.64 ± 0.18^b	(19)
		3.98 ± 0.19^c	
		4.02 ± 0.17^d	
PM2	45.4 ± 1.5		(19)
T7	51.2 ± 3.1		(19)
TMV	42.0 ± 2.0		(19)
T2	249 ± 20		(20)
		214^a	(108)
		234^a	(109)
		220^a	(110)
T4	213 ± 18		(20)
		192 ± 6^a	(111)
		203^a	(112)
T5	119 ± 9.5		(20)
		109.2 ± 4^a	(111)
λ	59.9		(20)

Note. Values obtained using other techniques are also given for comparative purposes.
[a] Differential Light Scattering.
[b] Sedimentation equilibrium.
[c] Sedimentation velocity.
[d] Sedimentation–diffusion.

able, albeit under-used, probe. Table I gives a comparison of molecular weights obtained by turbidimetry, compared with other methods. For example, Bahls and Bloomfield (20) have applied the technique to a range of bacteriophages (T2, T4, T5, and λ). After extrapolating the turbidities to zero concentration (to eliminate interparticle interference and thermodynamic nonideality effects) (Fig. 1) and assum-
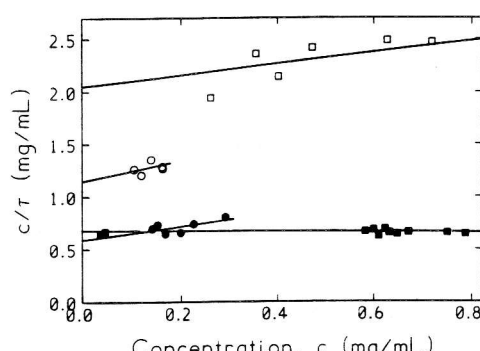
FIG. 1. Plots of c/τ, versus c (where τ is the turbidity and c the concentration) at 436 nm for bacteriophages T5 (O), T2 (●), λ (□), and T4 (■). Redrawn from (20).

ing that most of the scattering was due to the heads (which were assumed to be spherical) they obtained values for molecular weights to a precision and accuracy better than $\pm 10\%$, and in reasonable agreement with values from other techniques. Camerini-Otero et al. (22) claimed accuracies of up to $\pm 5\%$ for the viruses PM2, T7, R17, and TMV. (Both sets of measurements were obtained prior to the availability of the series method for obtaining Q.) Turbidimetry has also been used to investigate the behavior of TMV in mixed biopolymer systems (23). The accuracy by which molecular weights can be obtained is also dependent on the extent to which the particular spectrophotometer used will accept *scattered* light at low values of θ, which creates error. However, given the simplicity of measurement and the availability of spectrophotometers in biochemical laboratories it is surprising that the technique has not been more widely applied. It is to be hoped that the method will be used more frequently as the ease with which Q values can now be determined becomes more widely known.

2.2 Application to Bacteria

Turbidimetry has been applied to both the vegetative cells (21, 27) and spores of bacteria (24, 25), with the aim of (i) estimating the concentrations of microorganisms and (ii) estimating their masses. It is a particularly simple and useful technique for monitoring *changes* in numbers and masses.

Although bacteria normally scatter more strongly than viruses, theoretical interpretation of the data is more difficult since the limits of the RGD approximation—which assumes that phase changes of the scattered light are negligible—may be exceeded. This approximation is valid provided that the following condition is met:

$$\frac{4\pi n d}{\lambda_0}\left(\frac{n}{n_0} - 1\right) \ll 1 \qquad [9]$$

where d is the maximum dimension of the particle, n its refractive index, and n_0 the refractive index of the suspending medium. However, Koch (21) has pointed out that for vegetative bacterial cells this criterion may not be satisfied, because of the high refractility of the outer membrane, and for bacterial spores, the dehydrated protoplast. However, the major influence of the phase-shift is to the direction in which scattered wavelets most strongly interfere wihout influencing the *total* amount of interference and hence the turbidity (21). For bacteria, an equation equivalent to Eq. [3] and [4] has been used:

$$(\text{OD}) = \frac{\tau}{2.303} = \frac{32\pi^3(\partial n/\partial c)^2}{3\lambda_0^4}[q^2\nu]Q \qquad [10]$$

where ν is the number concentration of particles (ml^{-1}), q is the anhydrous mass of a single particle (g), and $q^2\nu \equiv M_r c/N_A$. For near-spherical bacteria, Q has been taken to be unity (21). This equation proves the truth of the general impression among bacteriologists (see, e.g., Ref. (26)) that turbidity is a more sensitive measure of the total mass or volume of bacteria in a sample than the number concentration. Thus it provides a very useful technique for monitoring the growth of bacteria. For example, Chung et al. (27) have used related techniques to study the effects of antibiotics on the growth of *Escherichia coli*.

Although the generalized treatment (which includes phase changes) known as the "Lorenz-Mie" theory is formidable—particularly for nonspherical particles—other approximations are available, such as that of Jobst (for large spheres only).

Koch (21) has used the RGD approximation to predict what the wavelength dependence ratio, $-d(\text{OD})/d \log \lambda_0$, would be for *E. coli*, based on a prolate ellipsoid of revolution of aspect ratio 4:1. His calculated value is in excellent agreement with the experimental value of 2.28 ± 0.02. Change in optical density with time has been widely used as a monitor for the extent of bacterial spore germination (see, e.g., (28, 29, 24, 25)). For dormant bacterial spores of *Bacillus subtilis,* Harding and Johnson (24) have shown that $-d \log(\text{OD})/d \log \lambda_0 = 0.89$ which is clearly lower than the value predicted by the RGD theory for a spore of modest asymmetry ($\approx 2{:}1$ aspect ratio). Thus the applicability of Eq. [10] was taken only tentatively and has so far been used only to give a *qualitative* indication of changes in mass of spores upon germination (24). This is consistent with the observation of Wyatt (personal communication) that Koch's treatment can only be modestly applied (1) to a single strain in a single growth medium (making it virtually impossible for comparing growth of different strains) and (2) when the culture is not a multiple scattering medium (i.e., for particle concentrations $\ll 10^7 \text{ ml}^{-1}$).

Finally Chernyak (60) has described how turbidity measurements can be used to study bacterial chemotaxis, in terms of the effects of attractants and repellents on concentrated suspensions of *E. coli.*

3. DIFFERENTIAL LIGHT SCATTERING

Although measurement of the total intensity loss through scattering of an incident beam can be relatively easy, much more valuable information can be obtained by examining the angular dependence of the amount of scattered light. This is most conveniently termed "differential light scattering." A typical light scattering photometer constructed for this purpose and the use of a laser light source have been described by Johnson and McKenzie (30). The advantages of lasers over traditional light sources are very high intensity, high collimation, and narrow spread of wavelength, which give much improved angular resolution in intensity envelopes (31): it is fair to say that in general the use of lasers has revolutionized the application of light scattering methods.

Interpretation of the scattering envelopes is largely dictated by the size of the particle. For example, most virus particles of M_r between $\approx 10^6$ and 10^8 are large enough for intraparticle interference effects between wavelets scattered from different points in the particle to be significant, yet small enough for there to be very little difference in phase between the wavelets scattered from the various points: hence the RGD approximation is valid.

3.1. Viruses

The basic equation for angular dependence of light scattering is written

$$\frac{Kc}{R_\theta} = \frac{1}{P(\theta)} \left\{ \frac{1}{M_r} + Bc \right\} \tag{11}$$

where $K = 2\pi^2 n_0^2 (\partial n/\partial c)^2 / N_A \lambda_0^4$; R_θ is the "Rayleigh ratio" and is given by R_θ
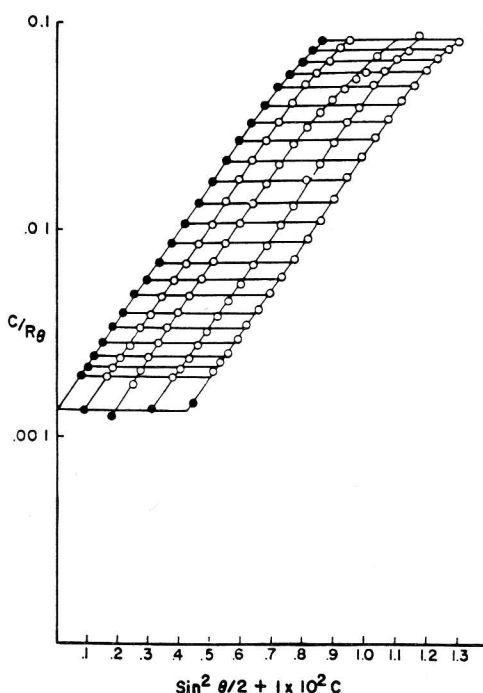
FIG. 2. Log Zimm plot of vaccinia virus for concentration ranges from $c = 0.88$–4.4 µg/ml. (- ○ -) Experimental points, (- ● -) extrapolated. Reproduced, by permission of the publisher, from Ref. (35).

$= (I_\theta r^2/(I_0(1 + \cos^2 \theta))$ where I_θ is the scattered intensity at scattering angle θ (viz., the angle between the incident and scattered radiation) and the other terms are as in section 2. The form taken by $P(\theta)$ will depend on the shape of the scattering particle— or, for flexible particles, on the average shape. For RGD scatterers, such as viruses,[2] $P(\theta)$ is related to the root mean square radius about the center of mass of the virus, R_g, by

$$P(\theta) = 1 - \frac{16\pi^2}{3\lambda^2} R_g^2 \sin^2 \left(\frac{\theta}{2}\right) + 0(\theta^2). \qquad [12]$$

R_g is almost ubiquitously referred to in the literature as an operational "Radius of Gyration," although this differs from its usage in a Classical Mechanical sense, where it is defined with respect to a fixed *axis of rotation*. However, providing its usage is consistent, no errors are introduced. This equation is the basis of the widely used biaxial extrapolation procedure of Zimm (32), and Fig. 2 shows an example of such a plot for vaccinia virus (35). Evidently to obtain M_r it is not only necessary to perform an extrapolation to zero concentration (as with turbidimetry) but also to zero angle. The slopes of both extrapolations (assuming they are linear) can be used to obtain respectively the second thermodynamic virial coefficient, B, and the radius of gyration, R_g. The common intercept gives $1/M_r$: a variety of virus molecular weights

---

[2] The validity of the RGD approximation for large rod-shaped virus particles such as TMV has been examined by Ravey (33).

TABLE II

Molecular Weights (Weight Averages) and Radii of Gyration for Various Microorganisms Obtained
Using Differential Light Scattering (e.g., by the "Zimm Plot" Technique)

	M_r	Mass (g)	R_g (nm)	Hydrodynamic diameter (nm)	Ref.
R17 virus	3.86×10^6		—	—	(121)
TMV	39×10^6		92.4	—	(113)
Vaccinia virus	$(2.7 \pm 2) \times 10^9$	$(4.5 \pm .3) \times 10^{-15}$	144 ± 2	373 ± 4	(35)
Serratia marcescens[a]	1.0×10^{11}	1.7×10^{-13}	340	880	(37)

[a] Infra-red radiation used.

and radii of gyration have been determined in this way (Table II). A general approach
is now available (34) whereby both R_g and B information can be used as a means of
determining the triaxial dimensions of viruses and other macromolecules using a
general ellipsoid model. This method does not require an estimate for particle solva-
tion, nor an initial estimate of the dimensions from, for example, electron micros-
copy. Finally, an interesting demonstration of the application of DLS to *polydisperse*
virus systems has been given by Wilzius (36), who showed that the particle length
distributions of TMV using DLS agreed with electron microscopy.

3.2 Application to Bacteria

From the nature of the scattering envelope, particularly including features at high
scattering angles (up to 180°), information concerning internal structure—in terms
of refractive index profiles—can be obtained by appropriate modeling of the form
factor $P(\theta)$—in terms of either RGD or generalized Mie scattering theory. The
"Zimm plot" method—based on the RGD approximation—has been successfully
applied to a bacterium (*Serratia marcescens*), but only by increasing the wavelength
of the radiation used into the infrared region (37).

Much of the theory for handling the DLS of large particles has been developed for
spherical scatterers (38), oriented ellipsoidal scatterers (39)—including the case of
variable refractive index (40)—ellipsoids in random orientations (41) and also poly-
disperse suspensions of ellipsoids (42). Despite these significant theoretical develop-
ments there are two major problems in attempting to use DLS for refractive index
profiling of vegetative cells or spores of bacteria:

1. Heterogeneity, viz., polydispersity/aggregation phenomena. This tends to ob-
scure any structural features in the angular intensity envelope making refractive in-
dex modeling impossible (43). This problem has been illustrated for suspensions of
B. subtilis spores by Harding and Johnson (24).

2. Asymmetry. Even if isolated particles *can* be examined, unless particles are
spherical the nature of the scattering profile will depend on particle orientation. Ran-
dom orientations of a suspension of monodisperse but asymmetric particles will also
tend to smooth out any structural features (44); this has also contributed to the ob-
scuring of structural features in Fig. 4 of Ref. (24).
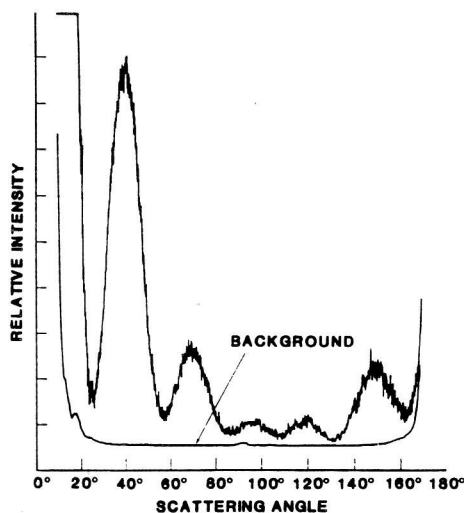
FIG. 3. DLS Intensity vs angle plot for a single spore of *B. sphaericus* suspended in an aerosol. Vertically polarized light used ($\lambda = 514.5$ nm). Reproduced, by permission of the publisher, from Ref. (44).

Considerable progress in tackling the problem of polydispersity was made by Wyatt and Phillips (44). An aerosol technique was used to suspend single particles in the laser beam, with the result that structural features in the intensity envelopes could be clearly seen (e.g., Fig. 3). The disadvantages are clear, however: (i) The relatively large refractive index difference between the cell and its nonaqueous environment means that the simple RGD theory is almost certainly not applicable, and hence Mie theory *must* be applied if refractive index profiles are to be modeled. (ii) Even for bacterial spores which have a rigid peptidoglycan cortex and which are already in a highly dehydrated state, the nonaqueous environment will lead to a refractive index profile that may be nonrepresentative of the spore in an aqueous environment. (iii) Vegeta-
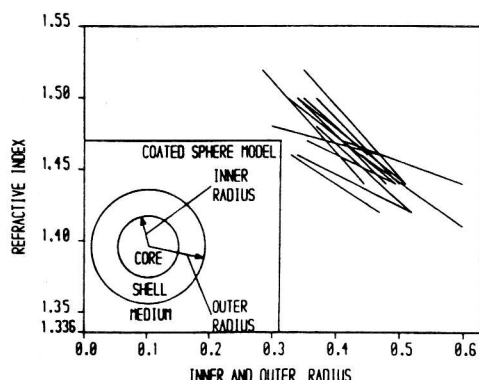
FIG. 4. Best-fit solutions for light scattering patterns from 16 individual dormant spores of *B. sphaericus* ATCC 9602. Each line represents one solution (best fit), the left hand end corresponding to the radius and the refractive index of the "core" and the right hand end to the outer "shell" of the coated sphere model (46).

tive forms are not in such a dehydrated state, have only a relatively thin peptidoglycan wall and no spore coat and hence the technique is not applicable.

More recently, however, significant progress has been made with a single particle solution differential photometer (45). Ulanowski *et al.* (46) have successfully modeled profiles for the "spherical" spores of *Bacillus sphaericus.* "Coated sphere" models were used, in which the radii of the outer spore coat and the inner radius of the cortex were used as variables; using generalized Mie theory for coated spheres they were able to model the internal structure for several spores of *B. sphaericus:* agreement between each individual spore examined was very good (Fig. 4). The application of this technique to more typical ellipsoidal spore particles will depend on the ability to orient the particle in the laser beam.

The theory developed for employing DLS techniques has found considerable application in antibiotic susceptibility testing: for rapidly determining the sensitivity of bacteria to drugs, and equipment has been specifically designed for this purpose (47–49). Recent applications to a wide range of bacterial systems have been described by Murray *et al.* (50) and Hukins *et al.* (51). Bateman (52) had earlier described how a fixed angle photometer could be used to monitor environmentally induced changes in bacteria, and McKie *et al.* (54) have applied this to determine the minimum inhibitory concentrations of antimicrobial agents.

4. QUASI-ELASTIC LIGHT SCATTERING (QLS)

This is probably a more difficult technique to apply than DLS, and the equipment is more expensive (primarily because of the cost of "autocorrelators") but directly yields information about the basic hydrodynamic properties (such as diffusion) of a system of microorganisms, and in particular *changes* that may occur therein. We have mentioned before how the specific properties of high intensity, high collimation, and narrow spread of wavelength of laser light sources have greatly enhanced the resolution of the scattering intensity profiles in DLS. However, it is the property of high coherence of laser radiation that has had the most significant impact, and this property has led to the rapid expansion of QLS techniques over the last decade. The basic principle is that, because of translational or rotational motions of particles in a suspension, the scattered intensity in a given direction will fluctuate with time. These intensity fluctuations can either be represented by a power spectrum $S(w)$ (this can be thought of as a "Doppler broadening" of the incident radiation) or more commonly in terms of an autocorrelation function $g^2(t)$. The dependence of $g^2(t)$ with time (or alternatively the dependence of $S(w)$ upon the wave number w) can be used to obtain (i) translational (or rotational) Brownian diffusion coefficients, (ii) an estimate for the polydispersity (through the "z-average variance" (125, 126), or, (iii) in the case of motile microorganisms, the distribution of particle velocities.

Godfrey *et al.* (55) have described how a conventional differential light scattering apparatus can be modified for QLS. An even fuller description of how such an apparatus can be constructed has been given by Sattelle and co-workers (127). The principal feature is an autocorrelator: a purpose-built digital computer which performs products of the intensity (as measured by the number of photons, n, received by a multiplier) at a time t with that at a succession of other times $t + b\tau$, typically for 128 or 256 values of b; τ is the sample time (not to be confused with the same symbol used for turbidity). The correlator evaluates the intensity autocorrelation function $g^2(t)$,
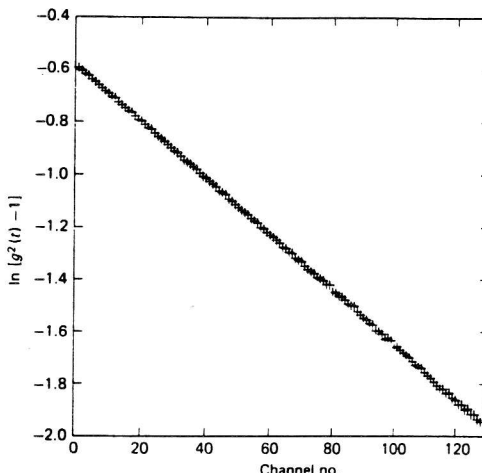
FIG. 5. Plot of $\ln[g^2(t) - 1]$ as a function of channel number for turnip yellow mosaic virus in phosphate/ NaCl buffer (66).

defined by $g^2(t) = \langle n(t)n(t + b\tau)\rangle/\langle n\rangle^2$ as a function of time, t, where the angled brackets denote an average over times long compared with τ. Commercial autocorrelators (62) which are integral with a microcomputer and software for many of the necessary analyses are now available. Alternatively, the data from the correlator may be stored and then transferred to a mainframe computer for full data analysis (24).

4.1. Application to Viruses

For dilute Brownian systems and where the effects of rotational diffusion are negligible in comparison with translational diffusion (such as for spherical viruses) $g^2(t)$ is related to the translational diffusion coefficient D_T by

$$[g^2(t) - 1]^{1/2} = e^{-D_T \mathbf{k} t} \tag{13}$$

where $\mathbf{k}$ is the Bragg wave vector defined by

$$\mathbf{k} = (4\pi n_0/\lambda_0)\sin\left(\frac{\theta}{2}\right).$$

Thus D_T can be found from a plot of $\ln[g^2(t) - 1]$ versus t. Figure 5 gives such a plot for a dilute suspension of Turnip Yellow Mosaic virus (TYMV). D_T values for other viruses obtained in this way are given in Table III. The sensitivity of QLS to virus structure has been clearly demonstrated by Baran and Bloomfield (56) who showed the effect of decreasing numbers of tail fibers on the D_T values of T4D bacteriophage. In further studies (57–60) Bloomfield and co-workers have taken advantage of the sensitivity of QLS measurements to analyze the kinetics of the T4 assembly process and the isomerization of T2L. Ohbayashi et al. (61) have also analyzed the T4 assembly process. Changes in the hydrodynamic properties associated with the onset of translation have been detected for Southern Bean Mosaic Virus by Brisco et al. (128).

A scattering angle of 90° is normally chosen for many QLS measurements, since stray scattering from dust particles, etc., become more of a problem at lower angles

TABLE III

Translational Diffusion Coefficient (D_T) Values for Microorganisms Determined by QLS

	Temp (°C)	D_T (cm² s⁻¹)	Hydrodynamic diameter (nm)	Ref.
B. subtilis spore	35	$(5.10 \pm .09) \times 10^{-9}$	1180	(24)
	25	$(4.20 \pm .07) \times 10^{-9}$	1180	(24)
B megaterium spore	35	$(5.01 \pm .10) \times 10^{-9}$	1200	(25)
	25	$(4.10 \pm .08) \times 10^{-9}$	1200	(25)
XF virus	20	$(2.53 \pm .06) \times 10^{-8}$		(71)
Fd virus	25	$(2.58 \pm .04) \times 10^{-8}$		(70)
TMV	20	3.2×10^{-8}		(114)
Potato virus X (PVX)	20	2.6×10^{-8}		(114)
M13 virus	20	2.6×10^{-8}		(114)
PF1 virus	20	1.4×10^{-8}		(114)
T2Lᵇ bacteriophage	20	3.13×10^{-8}		(115)
T2Lᵃ bacteriophage	20	2.12×10^{-8}		(115)
T2Lᵇ bacteriophage	20	3.53×10^{-8}		(57)
T2Lᵃ bacteriophage	20	3.05×10^{-8}		(57)
T4D bacteriophage	20	$(2.94 \pm .05) \times 10^{-8}$		(56)
φ NS11 virus	20	$(5.70 \pm .03) \times 10^{-8}$		(116)
T4D (Heads)	20	$(3.60 \pm .06) \times 10^{-8}$		(58, 59)
T4D (Tails)	20	6.0×10^{-8}		(59)
IPNV (Infectious Pancreatic Neurosis virus)	20	6.7×10^{-8}		(117)
Vesicular stomatis virus (Indiana)	20	$(2.69 \pm .10) \times 10^{-8}$		(118)
Vesicular stomatis virus (NJ)	20	$(2.68 \pm .10) \times 10^{-8}$		(118)
TYMV	20	$(1.42 \pm .01) \times 10^{-7}$	30.4	(66)
R17 virus	20	1.44×10^{-7}		(119)
		1.54×10^{-7}	140	(122)
MuLV virus	20	$(2.96 \pm .12) \times 10^{-7}$	145 ± 7	(120)
MuLV virus (in sucrose solvent)	20	$(2.78 \pm .05) \times 10^{-7}$	154 ± 3	(120)
AMV virus	20	$(3.19 \pm .07) \times 10^{-7}$	144 ± 3	(120)
AMV virus (in sucrose solvent)	20	$(3.11 \pm .09) \times 10^{-7}$	138 ± 4	(120)
MS2 virus	20	$(1.54 \pm .03) \times 10^{-7}$	140	(123)
Gipsy moth virus	20		176 ± 9	(124)
European pine sunflower virus	20		126 ± 6	(124)
Tipula iridescent virus	20		212 ± 10	(124)

Note. Values quoted are not necessarily "infinite dilution" values.

ᵃ Slow form—tail fibers stretched.

ᵇ Fast form—tail fibers folded back.

(56): clarification of solutions using appropriate ultrafilters is generally a necessity, especially for more asymmetric scatterers, where extrapolation to zero angle (to compensate for rotational diffusion effects) is necessary.

Although D_T values can be measured up to an accuracy of $\pm 0.2\%$ in this way, the value obtained directly from a plot of the form of Fig. 5 will be an *apparent* value because of the effects of thermodynamic nonideality. Extrapolation to zero concen-
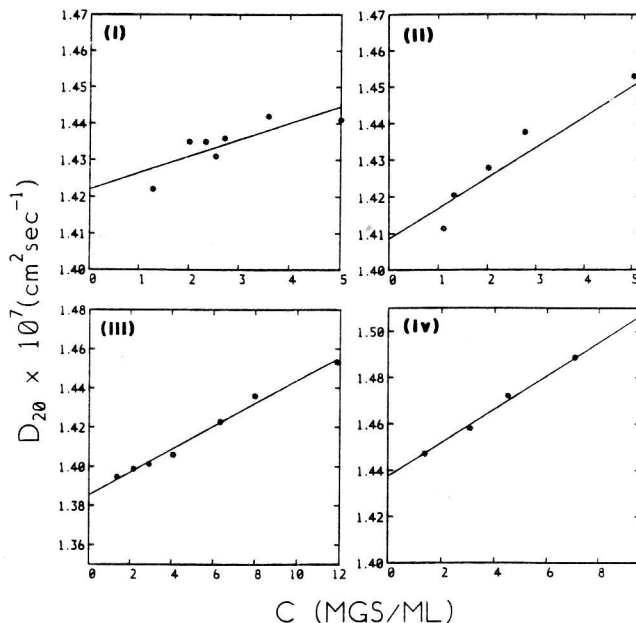
FIG. 6. Effect of solvent conditions on the concentration dependence of the apparent diffusion coefficient for TYMV. (i) pH 7.8, $I = 0.10$, (ii) pH 6.0, $I = 0.10$, (iii) pH 4.75, $I = 0.10$, (iv) pH 6.8, $I = 0.20$. All buffers phosphate–NaCl except (iii) (acetate).

tration is normally necessary: exact equations describing the concentration dependence are now available (63–65), and have been applied for a wide range of solvent conditions by Harding and Johnson (66) to TYMV; an illustration of the effect of solvent conditions on concentration dependence is given in Fig. 6.

For heterogeneous systems the diffusion coefficient so found will be a z-average diffusion coefficient. It can be combined in the standard way with the sedimentation coefficient (weight average) to yield a weight average M_r (see, e.g., Ref. (66)).

For nonspheroidal particles, rotational diffusion effects are no longer negligible and must be taken into consideration. In addition, Wilcoxon and Schurr (67) have pointed out that the anisotropy of the translational diffusion coefficient should be taken into account, and have offered this as an explanation of earlier discrepancies between QLS and other physicochemical measurements.

The relation corresponding to Eq. [13] for rod shape particles viz., when rotational effects are present, is (68)

TABLE IV

Rotational Diffusion Coefficient (D_R) Values Determined by QLS for Three Viruses

Virus	Temp (°C)	$D_R (s^{-1})$	Ref.
T4B phage	20	258 ± 12	(74)
T7 phage	20	4528 ± 100	(74)
TMV	20	323 ± 17	(73)

$$g^2(t) = 1 + A[1 + 2(B_2/B_0)\exp(-6D_R t) + \cdots]\exp(-2D_T k^2 t) \qquad [14]$$

where D_R is the rotational diffusion coefficient. A more general form for any optically anisotropic particle possessing cylindrical symmetry has been given by Aragon and Pecora (69) (see also Ref. (58)). Newman *et al.* (70) have pointed out that the ratio B_2/B_0 in Eq. [14], which depends on the rod length L (and hence the contribution from D_R), is negligible when $kL \rightarrow 0$; i.e., when D_T values obtained from Eq. [13] are extrapolated to zero angle as well as zero concentration. Alternatively D_R can be measured using some other suitable technique and then included in Eq. [14] from which D_T can be obtained without having to extrapolate to zero angle. This procedure has been adopted for Xf virus (71). One difficulty of this approach is that in Eq. [14] D_T will be an *apparent* diffusion coefficient, and hence the effective D_R *at that concentration* should be used.

D_R values themselves can be determined using QLS although this is in general *extremely difficult;* it has nonetheless been attempted for several viruses (Table IV) most notably TMV (72) and the filamentous fd virus (73). This has been achieved by curve fitting to equations of the form of Eq. [14]. D_R values for TMV have been determined using a cross-correlation technique by Kam and Rigler (75) using two detectors (see also Ref. (76)). Hopman *et al.* (74) have correctly pointed out the problem of double scattering effects in determining rotational diffusion coefficients (from the zero angle depolarization autocorrelation functions), and have provided a method for its minimization. They were able to obtain values for D_R of 4528 ± 100 s^{-1} and 255 ± 28 s^{-1} for bacteriophages T7 and T4B, respectively. The real disadvantages in QLS for obtaining rotational diffusion coefficients (as compared with transient electric birefringence) are that (i) the curve fitting procedures for equations of the form of Eq. [14] make it virtually impossible to take into consideration concentration dependence effects, which may not be negligible (77). (ii) In addition, for extended particles that are not strict rods, there will be up to three rotational diffusion coefficients (corresponding to rotation about the three principal axes in the particle). Electric birefringence decay can now be used to allow for this multiplicity of D_R, especially if other hydrodynamic data are used as constraints (78, 79). As a technique for measuring D_R values, QLS does possess the advantage, however, that the method is nonperturbative because high srength electric fields are not required (with the resulting requirement for low ionic strength solutions to minimize heating effects). It is also now possible to take into consideration flexibility effects in representing the observed correlation functions (Ref. (80) for fd virus).

4.2. Bacterial Spores

Knowledge of the structural factors responsible for the heat resistance of bacterial spores is of enormous commercial importance since all UHT and canning processes are designed to kill spores. Despite this urgent requirement and over 60 years of research the exact mechanisms which spores use to achieve such resistance remains to be determined. One of the problems is that most of the probes used hitherto (chemical, genetic, electron microscopy) have been destructive, viz., have perturbed the structure being investigated, or the structure has been masked (as with NMR). The value of QLS as a nondestructive probe has recently been demonstrated by application to dormant and germinating spores of *B. subtilis* (24) and *Bacillus megaterium*
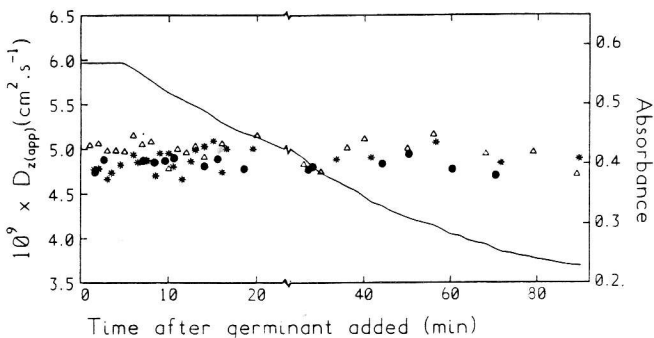
FIG. 7. Plot of diffusion coefficient (measured at a scattering angle of 90°) for *B. megaterium* spores, as a function of time after addition of germinant (L-alanine). The different symbols correspond to different runs. The continuous line represents a corresponding plot of turbidity (expressed in absorbance units at 580 nm) versus time. The temperature was 34.7°C and the concentration was 6×10^7 particles ml^{-1} (25).

(25). Apparent D_T values were determined for the dormant spore (Table III) and found to correspond to Stokes radii consistent with those found from electron microscopy. Little change in diffusion coefficient (and hence volume) was observed at the onset of germination (Fig. 7), apparently consistent with the Ellar theory (81) of spore heat resistance—that is, neither an expanded nor a contracted cortex is required for the onset of spore dehydration and resistance during dormancy. At longer times swelling of the protoplast occurred, again consistent with the observations of others using different techniques (28). Although QLS primarily gives information concerning the *gross* morphology, when combined with DLS measurements it can, in principle at least, be used to model the internal structure, based on "scaling profiles" of
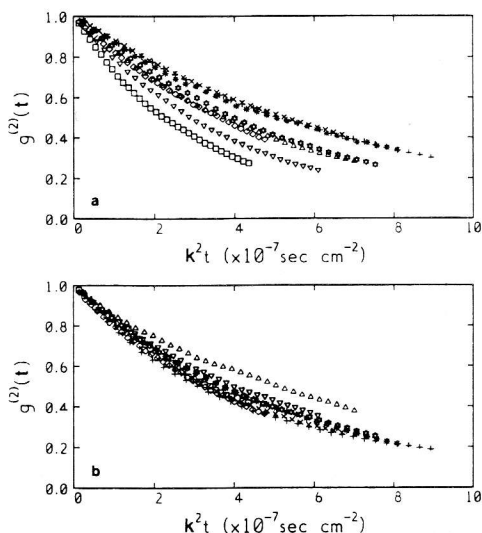
FIG. 8. Scaling plots for dormant (a) and germinated (b) spores of *B. megaterium*. The different symbols correspond to different scattering angles ranging from 8–90°. The better scaling of (b) is probably ascribable to a reduction in asymmetry of the germinated spore (25).
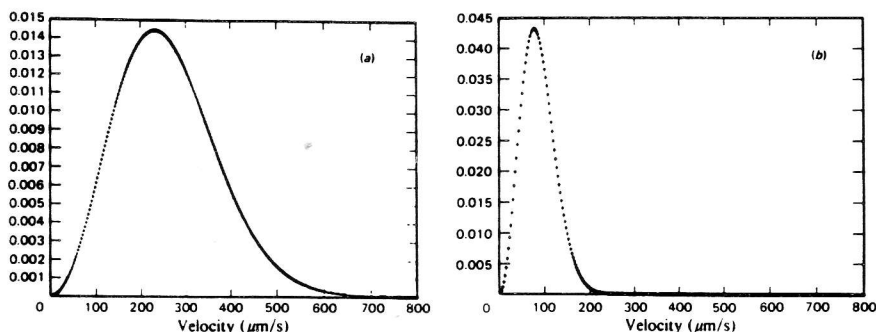
FIG. 9. Effect of Bromo-acetyl carnitine (BAC) on the velocity distribution of *T. brucei*, as determined by QLS (101, 102) (a) control, 282.0 μm/s root mean square velocity (rms), (b) 10 min after addition of BAC; 94.1 μm/s rms (102).

autocorrelation functions (40). This has already been applied to spores of *B. megaterium* (25) to give qualitative information about conformation changes during germination. The improved superposition of autocorrelation functions as a function of scattering angle θ of germinated spores (Fig. 8) can either be interpreted as the particles becoming less asymmetric or a greater homogeneity of the internal structure.

4.3. Motile Microorganisms

Besides being Brownian diffusers, many microorganisms (such as bacteria, cilliates, and flagellates) possess motility, driven by their own metabolism. One of the greatest successes of QLS has been its use as a rapid, noninvasive technique for the characterization of the velocity distributions of a wide range of microorganisms, from motile bacteria such as *E. coli* (82–87), spermatozoa (88–101) through to parasitic microorganisms such as *Trypanosoma brucei* (102, 103).

The general equation describing the intensity autocorrelation function of motile organisms of velocity V and velocity distribution $P(V)$ is

$$[g^2(t) - 1]^{1/2} = \int_0^\infty e^{i\mathbf{k} \cdot \mathbf{V}t} \cdot P(\mathbf{V})d^3\mathbf{V}. \qquad [15]$$

The particular form of this integral has been worked out for several types of distribution (see Refs. (81, 104, 105)). Expressions can be unwieldy but a particularly simplified form has been given by Chen and Hallett (104) for the case of particles with an isotropic Maxwellian distribution of velocities:

$$[g^2(t) - 1]^{1/2} = (1 - B)e^{-D_T k^2 t} + Be^{-k^2 V_{\text{rms}}^2 t^2/6} \qquad [16]$$

where B is the fraction of organisms that are motile and V_{rms} the root mean square velocity. D_T, V_{rms}, and B are normally obtained by nonlinear least-square fitting procedures to equations of the form of Eq. [16]. For helical motion, the instantaneous tangential speed is given by $V_T = (V_0^2 + \omega^2 R)^{1/2}$, where V_0 is the "progressive" speed and ω the helical angular velocity at a radius R.

It should be pointed out that for many systems the assumption of isotropicity in deriving Eq. [16] may be a poor one. An indication of the applicability is given by a

TABLE V

Light Scattering Techniques

Technique	Type of microorganism examined	What is measured experimentally	Other information required	Information obtained
Turbidimetry	(i) Any	Total loss in intensity through scattering	Refractive index increment	Molecular weight
	(ii) Motile	Total loss in intensity through scattering	Refractive index increment	Effects of environmental conditions on motility
Differential light scattering	(i) Virus	Angular dependence of scattered intensity	—	Molecular weight, radius of gyration, 2nd virial coefficient
	(ii) Spore	Angular dependence of scattered intensity	—	Refractive index profile of internal structure
Quasi-elastic light scattering	(i) Virus	Time resolved intensity fluctuations (TRIF)		Translational diffusion coefficient. Rotational diffusion coefficient
			Sedimentation coefficient.	Molecular weight
	(ii) Spore	Time resolved intensity fluctuations (TRIF)		Translational diffusion coefficient
		Angular dependence of TRIF		Asymmetry, internal structure
	(iii) Motile microorganisms	TRIF		Velocity distribution; effects of environmental conditions

"scaling procedure" developed by Stock (106)—viz., autocorrelation functions plotted versus kt for various values of k will superimpose for isotropic Maxwellian scatterers.[3] In this way Stock has demonstrated scaling for *Salmonella typhimurium*. For typical "nonscalers" Chen and Hallett (104) have attempted a model to fit progressive rotational and helical movements.

From scalers of one sort to scalers—viz., bacterial scale contamination in fermentation reactors—in a more chemical engineering sense, Slater *et al.* (107) have used the technique to investigate the ability of *Bacillus cereus* to migrate counter to a hydrodynamic gradient. Using equations of the form of Eq. [16] and assuming an isotropic velocity distribution they obtained values of D_T of $(4.6 \pm 0.2) \times 10^{-9}$ cm^2 s^{-1} for nonmotile bacteria and a mean value of $(3.6 \pm 0.3) \times 10^{-6}$ cm^2 s^{-1} for motile bacteria.

---

[3] This is analogous to scaling plots for pure Brownian diffusion (Fig. 8) where k^2t is used.
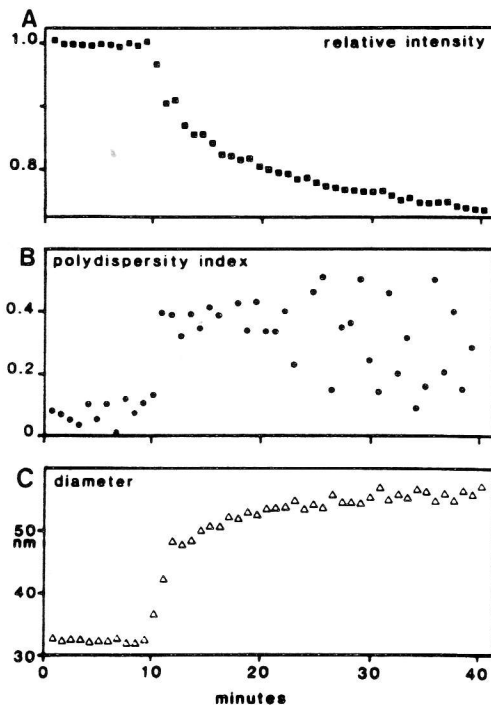
FIG. 10. Effect of removal of Ca^{2+} (by adding EGTA at time t = 10.5 min) on southern bean mosaic virus. (A) Intensity of scattered light (arbitrary units). (B) Polydispersity index (arbitrary units). (C) Hydrodynamic Diameter (nm) computed from D_T measured by QLS (from (128)).

QLS has been widely applied to the study of sperm motility measurements (88–101) and has permitted the testing of a range of media for their capacity to support sperm activity *in vitro* (cf. Sattelle *et al.* (101)).

Another interesting example of motility analysis has been to illustrate the effect of bromo-acetyl carnitine (BAC) on the motility of *T. brucei* (102, 103), a single-celled parasite that causes sleeping sickness in humans. Klein and co-workers were able to monitor the effects of BAC by following the dramatic changes in velocity distribution as a function of time after its addition (Fig. 9).

This latter application of a particular type of light scattering technique—QLS— would therefore appear somewhat related to the use of another type of measurement—DLS—for antibiotic susceptibility testing (47–52). A combined approach would therefore be fruitful for studies on similar systems in the future. Indeed, the three techniques described in this review—turbidimetry, DLS, and QLS—can give complementary information on a particular microbial system, whether it be on bacteria, bacterial spores, or virus structure (Table V); for example, the studies on bacterial spores (24, 25) and the work of Brisco *et al.* on the kinetics of swelling of southern bean mosaic virus (128). The latter study demonstrates the significance of recording turbidity, translational diffusion coefficient, and polydispersity information simultaneously (Fig. 10). However, in general it is fair to say that such a "combined" light scattering approach has not been frequently adopted. Nonetheless, it is my opinion that the way forward is to apply more than one of the light scattering methods to a

particular microbial system, in conjunction with other techniques such as electron microscopy, electric birefringence, and analytical ultracentrifugation, wherever appropriate.

ACKNOWLEDGMENTS

REFERENCES

1. TANFORD, C. (1961) Physical Chemistry of Macromolecules, pp. 302–307. Wiley, New York.
2. VAN DE HULST, H. C. (1957) Light Scattering by Small Particles. Wiley, New York.
3. STACEY, K. A. (1956) Light Scattering in Physical Chemistry, Academic Press, New York.
4. KERKER, M. (1969) The Scattering of Light and other Electro-magnetic Radiation, Academic Press, New York.
5. PITTZ, E. P., LEE, J. C., BABLOUZIAN, B., TOWNEND, R., AND TIMASHEFF, S. N. (1973) in Methods in Enzymology (Hirs, C. H. W., and Timasheff, S. N., eds.), Vol. 27, p. 209, Academic Press, Orlando, Fla.
6. BERNE, B. J., AND PECORA, R. (1976) Dynamic Light Scattering: With Applications to Biology, Chemistry and Physics, Wiley, New York.
7. CHU, B. (1974) Laser Light Scattering, Academic Press, New York.
8. KRATOHVIL, J. P. (1964) *Anal. Chem.* **36,** 458R–472R.
9. JOHNSON, P. (1985) *J. Surf. Sci. Technol.* **1,** 73–85.
10. CHEN, S. H., AND NURMIKKO, A. V. (1974) in Spectroscopy of Biology and Chemistry: Neutron, X-ray, Laser (Chen, S. H. ed.), Academic Press, New York.
11. BERNE, B. J., AND PECORA, R. (1974) *Annu. Rev. Phys. Chem.* **25,** 233–253.
12. BLOOMFIELD, V. A., AND LIM, T. K. (1978) in Methods in Enzymology (Hirs, C. H. W., and Timasheff, S. N., eds.), Vol. 48, Pt. F, pp. 415–494. Academic Press, Orlando, Fla.
13. SCHURR, J. M. (1977) *Crit. Rev. Biochem.* **4,** 371–431.
14. KRAUSE, S. J. (ed.) (1981) Molecular Electro Optics, Plenum, New York.
15. RIMAI, L., SALMEEN, I., HART, D., LIEBES, L., RICH, M. A., AND MCCORMICK, J. J. (1975) *Biochemistry* **14,** 4621–4627.
16. TINOCO (1983) *Trends Biochem. Sci.* **8,** 41–44.
17. DOTY, P., AND STEINER, R. F. (1950) *J. Chem. Phys.* **18,** 1211–1220.
18. DEBYE, P. (1947) *J. Phys. Colloid Chem.* **51,** 18–32.
19. CAMERINI-OTERO, R. D., FRANKLIN, R. M., AND DAY, L. A. (1974) *Biochemistry* **13,** 3763–3773.
20. BAHLS, D. M., AND BLOOMFIELD, V. A. (1977) Biopolymers **16,** 2797–2799.
21. KOCH, A. L. (1961) *Biochim. Biophys. Acta* **51,** 429–441.
22. CAMERINI-OTERO, R. D., AND DAY, L. A. (1978) *Biopolymers* **17,** 2241–2249.
23. PREISS, J. W. (1976) *J. Chem. Phys.* **65,** 2913–2914.
24. HARDING, S. E., AND JOHNSON, P. (1984) *Biochem. J.* **220,** 117–123.
25. HARDING, S. E., AND JOHNSON, P. (1986) *J. Appl. Bacteriol.* **60,** 227–232.
26. KOCH, A. L. (1955) *J. Biol. Chem.* **217,** 931.
27. CHUNG, S. S., DRUGEON, H. B., REYNAUD, A., AND COURTIEU, A. L. (1982) *Ann. Microbiol. (Paris)* **133A,** 409–416.
28. GOULD, G. W. (1969) in The Bacterial Spore (Gould, G. W., and Hurst, A., eds.), p. 397, Academic Press, New York.
29. LEFEBVRE, G. M., AND ANTIPPA, A. F. (1985) in FEMS Symposium No. 18: Fundamental & Applied Aspects of Bacterial Spores (Dring, G. J., Ellar, D. J., and Gould, G. W., eds.), pp. 309–316, Academic Press, New York.
30. JOHNSON, P., AND MCKENZIE, G. H. (1977) *Proc. R. Soc. B.* **199,** 263–278.
31. JOHNSON, P. (1984) *Biochem. Soc. Trans.* **12,** 623–625.
32. ZIMM, B. H. (1948) *J. Chem. Phys.* **16,** 1093–1099.
33. RAVEY, J. C. (1977) *J. Polym Sci. Polym. Symp.* **61,** 129–138.
34. HARDING, S. E. (1986) Submitted for publication; see also HARDING, S. E. (1986) *Macromolecular Preprints* **86,** 145.

35. FIEL, R. J., MARK, E. H., AND MUNSON, B. R. (1970) *Arch. Biochem. Biophys.* **141**, 547–551.
36. WILZIUS, P. (1982) *Appl. Opt.* **21**, 2022–2026.
37. MORRIS. V. J., COLES, H. J., AND JENNINGS, B. R. (1974) *Nature (London)* **249**, 240–241.
38. WYATT, P. J. (1962) *Phys. Rev.* **127**, 1837–1843; *Ibid* errata (1964) **134**, ABI.
39. ASANO, S. (1979) *Appl. Opt.* **18**, 712–723.
40. CHEN, S. H., HOLZ, M., AND TARTAGLIA (1977) *Appl. Opt.* **16**, 187–194.
41. BARBER. P. W., AND MASSOUDI, H. (1982) *Aerosol Sci. Med. Technol.* **1**, 303–315.
42. WANG, D. S., CHEN, H. C. H., BARBER, P. W., AND WYATT, P. J. (1979) *Appl. Opt.* **18**, 2672–2678.
43. WYATT, P. J. (1973) *Methods Microbiol.* **8**, 183–263.
44. WYATT, P. J., AND PHILLIPS, D. T. (1972) *J. Colloid Interface Sci.* **39**, 125–135.
45. LUDLOW, I. K., AND KAYE, P. H. (1979) *J. Colloid Interface Sci.* **69**, 571–589.
46. ULANOWSKI, J., LUDLOW, I., AND WAITES, W. F. (1986) Unpublished results.
47. STULL. J. (1973) *Clin. Chem.* **19**, 883–890.
48. WYATT, P., STULL, J., VINCENT, R., PROCTOR, W. L.. AND MILLER, I. L. (1978) Brit. GB 1515681, 28 Jun 1978; see also WYATT, P. J. (1980) *Gov. Rep. Announce. Index (U.S.)* **80**, 1287.
49. WYATT, P. J. (1975) *Autom. Microbiol. Immunol. [Pap. Symp.]*, Meeting Date 1973, 267–291.
50. MURRAY, J., EVANS, P., AND HUKINS, D. W. L. (1980) *J. Clin. Pathol.* **33**, 995–1001.
51. HUKINS, D. W. L., MURRAY, J., AND EVANS, P. (1980) *UV Spectrom. Group Bull.* **8**, 18–28.
52. BATEMAN, J. B. (1968) *J. Colloid Interface Sci.* **27**, 458–474.
53. WYATT, P. J. (1980) *Gov. Rep. Announce. Index (U.S.)* **80**, 1287.
54. MCKIE. J. E., SEO, J., AND ARVESEN, J. N. (1980) *Antimicrob. Agents Chemother.* **17**, 813–823.
55. GODFREY, R. E., JOHNSON, P., AND STANLEY, C. J. (1982) *in* Biomedical Applications of Laser Light Scattering (Sattelle, D. B., Lee, W. I., and Ware, B. R., eds.), pp. 373–389, Elsevier, Amsterdam.
56. BARAN, G. J., AND BLOOMFIELD, V. A. (1978) *Biopolymers* **17**, 2015–2028.
57. WELCH, J. B., AND BLOOMFIELD, V. A. (1978) *Biopolymers* **17**, 2001–2014.
58. BENBASAT, J. A., AND BLOOMFIELD, V. A. (1975) *J. Mol. Biol.* **95**, 335–357.
59. BENBASAT, J. A., AND BLOOMFIELD, V. A. (1981) *Biochemistry* **20**, 5018–5025.
60. CHERNYAK, B. V. (1982) *FEMS Microbiol. Lett.* **13**, 113–116.
61. OHABAYASHI, K., MINODA, M., AND UTIYAMA, H. (1981) **14**, 1031–1034.
62. For example, Malvern Instruments (1985) 4700 Documentation. PB041 2-85.
63. BATCHELOR, G. K. (1976) *J. Fluid Mech.* **74**, 1–29.
64. BATCHELOR, G. K. (1982) *J. Fluid Mech.* **119**, 379–408.
65. HARDING, S. E., AND JOHNSON, P. (1985) *Biochem. J.* **231**, 543–547.
66. HARDING, S. E., AND JOHNSON, P. (1985) *Biochem. J.* **231**, 549–555.
67. WILCOXON, J., AND SCHURR, J. M. (1983) *Biopolymers* **22**, 849–867.
68. PECORA, R. (1964) *J. Chem. Phys.* **40**, 1604–1614.
69. ARAGON, S. R., AND PECORA, R. (1977) *J. Chem. Phys.* **66**, 2506–2516.
70. NEWMAN, J., SWINNEY, H. L., AND DAY, L. A. (1977) *J. Mol. Biol.* **116**, 593–606.
71. CHEN, F. C., KOOPMANS, G., WISEMAN, R. L., DAY, L. A., AND SWINNEY, H. L. (1980) *Biochemistry* **19**, 1373–1376.
72. BERKOWITZ, S. A., AND DAY, L. A. (1976) *J. Mol. Biol.* **102**, 531–547.
73. THOMAS, J. C., AND FLETCHER, G. C. (1978) *Biopolymers* **17**, 2755–2756.
74. HOPMAN, P. C., KOOPMANS, G., AND GREVE, J. (1980) *Biopolymers* **19**, 1241–1255.
75. KAM, Z., AND RIGLER, R. (1982) *Biophys. J.* **39**, 7–13.
76. GRIFFIN, W. G., AND PUSEY, P. N. (1979) *Phys. Rev. Lett.* **43**, 1100–1104.
77. RIDDIFORD, C. L., AND JENNINGS, B. R. (1967) *Biopolymers* **5**, 757–771.
78. HARDING, S. E., AND ROWE, A. J. (1983) *Biopolymers* **22**, 1813–1829.
79. HARDING, S. E. (1986) *Biochem. Soc. Trans.* **14**, 857–858.
80. FUJIME, S., AND MAEDA, T. (1985) *Macromolecules* **18**, 191–195.
81. ELLAR, D. J. (1978) *Symp. Soc. Gen. Microbiol.* **28**, 295–325.
82. NOSSAL, R., AND CHEN, S. H. (1972) *Opt. Commun.* **51**, 117–122.
83. NOSSAL, R., AND CHEN, S. H. (1973) *Nature (London)* **244**, 253–254.
84. SCAHEFER, D. W., AND BERNE, B. J. (1975) *Biophys. J.* **15**, 785–794.
85. HOLZ, M., AND CHEN, S. H. (1978) *Appl. Opt.* **17**, 1930–1937.
86. WANG, P. C., AND CHEN, S. H. (1981) *Biophys. J.* **36**, 203–219.
87. CHEN, S. H., AND WANG, P. C. (1982) *in* Biomedical Applications of Laser Light Scattering (Sattelle, D. B., Lee, W. I., and Ware, B. R., eds.), Elsevier, Amsterdam.

88. BERGE, P., VOLOCHINE, B., BILLARD, R., AND HAMELIN, A. (1967) *C. R. Acad. Sci. (Paris)* **265**, 889–892.

89. NOSSAL, R. (1971) *Biophys. J.* **11**, 341–354.

90. DUBOIS, M., JOUANNET, D., BERGE, P., VOLOCHINE, N., SERRES, C., AND DAVID, G. (1975) *Ann. Phys. Biol. Med.* **9**, 19–41.

91. LEE, W. I., AND VERDUGO, P. (1976) *Biophys. J.* **16**, 1115–1119.

92. MATSUMOTO, G., SHIMITZU, H., SHIMADA, J., AND WADA, A. (1977) *Opt. Commun.* **22**, 369–373.

93. HALLETT, F. R., CRAIG, T., AND MARSH, J. (1978) *Biophys. J.* **21**, 203–216.

94. FINSY, R., PEETERMANS, J., AND LEKKERKERKKER, H. (1979) *Biophys. J.* **27**, 187–192.

95. CRAIG, T., HALLETT, F. R., AND NICKEL, B. (1979) *Biophys. J.* **28**, 457–472.

96. HARVEY, J. D., AND WOODFORD, M. W. (1980) *Biophys. J.* **31**, 147–156.

97. RACEY, T. J., HALLETT, F. R., AND NICKEL, B. (1981) *Biophys. J.* **35**, 557–571.

98. CRAIG, T., HALLETT, F. R., AND CHEN, S. H. (1982) *Appl. Opt.* **21**, 648–653.

99. HALLETT, F. R. (1982) *in* Biomedical Applications of Laser Light Scattering (Sattelle, D. B., Lee, W. I., and Ware, B. R., eds.), Elsevier, Amsterdam.

100. LEE, W. I. (1982) *in* Biomedical Applications of Laser Light Scattering (Sattelle, D. B., Lee, W. I., and Ware, B. R., eds.), Elsevier, Amsterdam.

101. SATTELLE, D. B., PALMER, G. R., AND DOTT, H. (1985) *Eur. J. Biophys.* **11**, 203–210.

102. GILBERT, R. J., KLEIN, R. A., AND JOHNSON, P. (1983) *Biochem. Pharmacol.* **32**, 3447–3451.

103. KLEIN, R. A. (1984) *Biochem. Soc. Trans.* **12**, 629–630.

104. CHEN, S. H., AND HALLETT, F. R. (1982) *Q. Rev. Biophys.* **15**, 131–222.

105. STOCK, G. B. (1978) *Biophys. J.* **22**, 79–96.

106. STOCK, G. B. (1976) *Biophys. J.* **16**, 535.

107. SLATER, N. K. H., POWELL, M. S., AND JOHNSON, P. (1981) *Trans. Indian Inst. Chem. Eng.* **59**, 170–176.

108. CUMMINGS, D. J., AND KOZLOFF, L. M. (1960) *Biochim. Biophys. Acta* **44**, 445–458.

109. BENDET, I. J., SWABY, L. G., AND LAUFFER, M. A. (1957) *Biochim. Biophys. Acta* **25**, 252–262.

110. TAYLOR, N. W., EPSTEIN, H. T., AND LAUFFER, M. A. (1955) *J. Amer. Chem. Soc.* **77**, 1270–1273.

111. DUBIN, S. B., BENEDEK, G. B., BANCROFT, F. C., AND FRIEFELDER, D. (1970) *J. Mol. Biol.* **54**, 547–556.

112. WELCH, J. B. (1976) PhD Thesis, University of Minnesota.

113. BOEDTKER, H., AND SIMMONS, N. S. (1958) *J. Amer. Chem. Soc.* **80**, 2550.

114. LOH, E., RALSTON, E., AND SCHUMAKER, V. N. (1979) *Biopolymers* **18**, 2549–2567.

115. HOPMAN, P. C., AND KOOPMANS, G. (1979) *Biopolymers* **18**, 1551–1553.

116. SAKAI, Y., MAEDA, T., AND OSHIMA, T. (1979) *J. Biochem. (Tokyo)* **85**, 1205–1211.

117. DOBOS, P., HALLETT, R., KELLS, D. T. C., SORENSEN, O., AND ROWE, D. (1977) *J. Virol.* **22**, 150–159.

118. HARTFORD, S. L., LESNAW, J. A., FLYGARE, W. H., MacLEOD, R., AND REICHMANN, M. E. (1975) *Proc. Natl. Acad. Sci. USA* **72**, 1202–1205.

119. LOWENSTEIN, M. A., AND BIRNBOIM, M. H. (1975) *Biopolymers* **14**, 419–430.

120. SALMEEN, I., RIMAI, L., LIEBES, L., RICH, M. A., AND McCORMICK, J. J. (1975) *Biochemistry* **14**, 134–141.

121. CAMERINI-OTERO, R. D. (1973) PhD Thesis, New York University.

122. CAMERINI-OTERO, R. D., PUSEY, P. N., KOPPEL, D. E., SCHAEFE, D. W., AND FRANKLIN, R. M. (1974) *Biochemistry* **13**, 96–970.

123. NIEUWENHUYSEN, P., AND CLAUWAERT, J. (1977) *Biopolymers* **17**, 2039–2040.

124. DEBLOIS, R. W., UZGIRIS, E. E., CLUXTON, D. H., AND MAZZONE, H. M. (1978) *Anal. Biochem.* **90**, 273–288.

125. KOPPEL, D. E. (1972) *J. Chem. Phys.* **11**, 4814–4820.

126. PUSEY, P. (1974) *in* Photon Correlation & Light Beating Spectroscopy (Cummins, H. Z., and Pike, E. R., eds.), pp. 387–428, Plenum, New York.

127. SATTELLE, D. B., PALMER, G. R., GRIFFIN, M. C. A., AND HOLDER, R. E. D. (1982) *Med. Biol. Eng. Comput.* **20**, 37–43.

128. BRISCO, M., HANIFF, C., HULL, R., WILSON, T. M. A., AND SATTELLE, D. B. (1986) *Virology* **148**, 218–220.